

IMAGE RESTORATION OF MEDICAL IMAGES WITH STREAKING ARTIFACTS BY EULER'S ELASTICA INPAINTING

Xiaochen Zhang, Justin W.L. Wan

University of Waterloo
Centre for Computational Mathematics in Industry and Commerce, and
David R. Cheriton School of Computer Science
200 University Avenue West, Waterloo, ON N2L 3G1, Canada

ABSTRACT

Streaking artifacts caused by metallic objects severely affect the visual quality of CT images, resulting in medical misdiagnosis. Commonly used approaches for metal artifact reduction usually consist of interpolation and iterative methods. The former one tends to lose image quality by introducing extra artifacts, while the latter is more computationally expensive. This paper proposes a new approach based on the Euler's elastica inpainting technique, which can preserve sharp edges and curvature when reconstructing the sinogram image, resulting in better quality in the restored CT image. Results of quantitative and qualitative experiments on both simulated phantoms and clinical CT images demonstrate that our method can suppress metal artifacts significantly.

Index Terms— Metal artifact reduction, CT image, Euler's elastica inpainting, numerical interpolation methods.

1. INTRODUCTION

Streaking artifacts caused by unavoidable metallic objects inside the scanning body largely degrade the quality of computed tomography (CT) images, causing challenges to medical diagnosis. They commonly appear in the dental fillings, cardiac pacemakers and knee prostheses. The formation of artifacts has multiple mechanisms, including beam hardening, scatter, noise, motion and edge effects [1]. Among those, beam hardening is one of the most prominent sources. High-attenuating metallic materials disturb the propagation of polychromatic X-ray beams when passing through the examining materials, and few photons can be detected. After the filtered backprojection (FBP) reconstruction, these missing data result in severe artifacts around metal regions on the reconstructed image as shown in Fig. 1.

There are two main categories for metal artifact reduction (MAR): projection completion methods, and statistical iterative methods. The main idea of projection completion methods is to replace the corrupted pixels in the raw data with proper values calculated from the surrounding information. The specific approaches used for prediction are various,

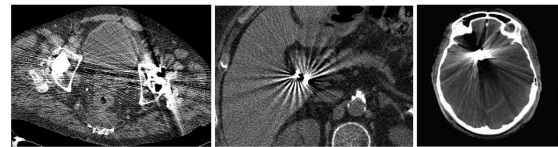


Fig. 1. Examples of streaking artifacts in CT images

such as linear interpolation [2], cubic interpolation [3], polynomial interpolation [4], and wavelet interpolation [5]. Moreover, image preprocessing techniques have been introduced. One of the successful methods, called normalized MAR, is to make use of a prior image acquired from a segmentation of the tissues [6]. Conventional projection completion methods are straightforward and fast; however, one of the significant drawbacks is that the inconsistency and inaccurate interpolation values could result in new artifacts after reconstruction. Statistical iterative approaches achieve better restoration performance [7]. However, due to their extremely high computational cost [1], most MAR methods belong to the first category.

In this paper, we present a novel approach using Euler's elastica inpainting for metal artifacts reduction. The proposed method belongs to the projection correction MAR category. However, instead of using conventional 1-D interpolation, our key idea is to use Euler's elastica inpainting which is essentially a 2-D interpolation that better preserves sharp edges and curvature features of the sinogram image, thus making the restoration results more continuous and smooth. Experiments in this paper show that Euler's elastica inpainting yields better results than 1-D interpolation in filling the corrupted regions of the sinogram and largely improves the visual quality of the artifact-polluted CT images.

2. METHODOLOGY

The main cause of the streak artifact is due to incomplete data of the sinogram as a result of the metal obstruction inside the body. When examining the sinogram image, the in-

complete data forms traces due to the metal object that typically have very different (and incorrect) values compared to the surrounding areas. Our proposed method is to identify the corrupted regions (metal trace) and then fix the values by an image inpainting technique.

More specifically, the method consists of the following steps. First, the metal is segmented from the initial artifact image, followed by a forward projection. The metal sinogram is then compared with the original sinogram to locate the metal trace. Before implementing the inpainting algorithm, a contrast enhancement technique is applied. Then the inpainted sinogram is reconstructed back into a 2-D image. If necessary, an iterative correction is applied until convergence. A flowchart of the whole procedure is as shown in Fig. 2. Each

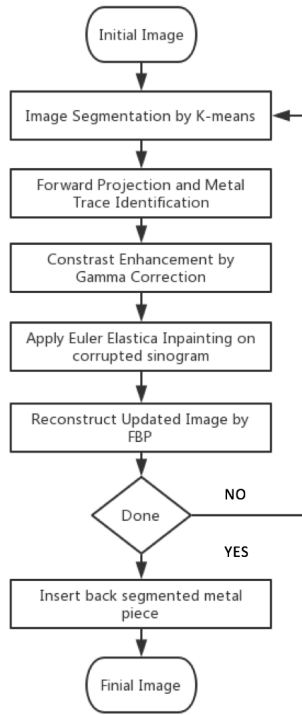


Fig. 2. Flowchart of the whole methodology

step of the method is described in more details in the following sections.

2.1. Metal Segmentation

In the first step, metal parts are separated from the original image by either thresholding, or other image segmentation methods. When artifacts are intense, simple threshold does not perform well. Here, we apply K-means clustering algorithm to separate the initial image into different parts according to their density. K-means clustering is an algorithm to classify the objects into K clusters by minimizing their distance to the centroid point. In general, K can be selected manually or randomly. Since we just separate the image into

metal and non-metal regions, $K = 2$ would be the first choice. However, when the image is more complicated, we often use larger K to classify the image into several clusters according to the tissue's density and then manually choose the metal one.

2.2. Forward Projection and Metal Trace Identification

After segmentation, a forward projection is applied to the segmented metal pieces to obtain a metal mask. Comparing the metal mask with the original sinogram, we can locate the metal trace, which is needed to determine the inpainting domain in following steps. Normally, the inpainting domain is set slightly larger than the computed metal trace. We use a σ parameter to control the thresholding, and $S(i, j)$ is the value at pixel (i, j) :

$$Mask_{metal}^k = \begin{cases} 1, & \text{if } S(i, j) \geq \sigma, \\ 0, & \text{if } S(i, j) < \sigma. \end{cases} \quad (1)$$

2.3. Contrast Enhancement

Since sinograms are normally low-contrast gray-scale images, a preprocessing step is added to increase the contrast before inpainting. Higher contrast corresponds to larger gradient values, so that curvature can be captured more accurately. Accordingly, when inpainting is completed, an inverse correction is applied to restore the original contrast. The standard Gamma Correction method is used, which is defined as:

$$V_{out} = A \cdot V_{in}^\gamma \quad (2)$$

where A is a constant, V_{in} is the input, and V_{out} is after-processing output.

2.4. Sinogram Inpainting

The objective of the image inpainting problem is to fill in the missing regions of an image with proper values, so that the whole image looks natural to human eyes [7]. In contrast to the standard interpolation methods where only one-dimensional information is used, inpainting allows information from neighborhoods of all directions to recover intensity values in the missing regions, often referred to as the inpainting domain. In this paper, we will apply the Euler's elastica inpainting [8] to restore values in the corrupted metal trace.

The elastica function originally describes the energy stored in a flexible rod when it is clamped in two directions. This inpainting model tries to find a curve, Γ , that minimizes the elastica function defined as follows:

$$E[\Gamma] = \int_{\Gamma} (a + b\kappa(s)^2) ds, \quad (3)$$

where $\kappa(s)$ is the curvature of the curve, a , b are two positive constants, and the ratio of b/a determines the elastica of the curve.

Referring to Fig. 3, the entire region is Ω . The original image is $u(x)$, $x \in \Omega$ and $x \in D$ are the missing pixels to be inpainted based on the available value in the extended region E .

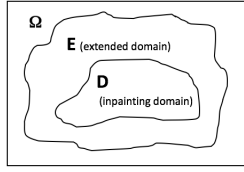


Fig. 3. The inpainting domain and the extended domain are denoted by D and E , respectively.

The curvature of u can be computed by the divergence of the normal, i.e. $\nabla \cdot \frac{\nabla u}{|\nabla u|}$, and $ds = \nabla u dx$. Thus the elastica energy function in the inpainting domain can be written as

$$E[u] = \int_D (a + b(\nabla \cdot \frac{\nabla u}{|\nabla u|})^2) |\nabla u| dx. \quad (4)$$

In order to avoid dramatic changes in intensity, a second fitting term is added to penalize any changes from the original image outside the inpainting domain. Also in practice, we apply the energy function on $E \cup D$ instead of only D to ensure smoother inpainting. The final energy function of Euler's elastica inpainting is

$$J[u] = \int_{E \cup D} (a + b(\nabla \cdot \frac{\nabla u}{|\nabla u|})^2) |\nabla u| dx + \frac{\lambda}{2} \int_E (u - u^0)^2 dx, \quad (5)$$

where u^0 is the given image, λ is the Lagrangian multiplier which controls the weight between the inpainting term and the fitting term. In [9], the authors show that solving (5) is equivalent to computing the steady state solution of the following equation:

$$\frac{\partial u}{\partial t} = |\nabla u| \nabla \cdot \vec{V} - |\nabla u| \lambda_E (u - u^0), \quad (6)$$

where

$$\vec{V} = (a + b\kappa^2) \vec{n} - \frac{2b}{|\nabla u|} \frac{\partial(\kappa |\nabla u|)}{\partial \vec{t}}, \quad \lambda_E = \begin{cases} \lambda, & u \in E, \\ 0, & u \in D. \end{cases}$$

Here, \vec{t} is the tangential direction and \vec{n} is the normal direction. We then use an unconditionally stable implicit scheme [10] to discretize the equation above and compute the solution numerically.

We note that since Euler's elastica inpainting incorporates curvature in the model, it prefers inpainting solutions to have small curvature, thus eliminating solutions with discontinuities and corners. Consequently, the model can produce smooth, continuous, and natural looking inpainting results. Moreover, results given by Euler's elastica inpainting satisfy the "connectivity principle", which enables the occluded edges and junctions to be connected smoothly even over a large gap [9].

2.5. Reconstruction

The inpainted sinogram is then reconstructed into a 2-D image by the filtered backprojection (FBP) algorithm, or inverse Radon transformation, after applying the inverse Gamma Correction.

2.6. Iterative Correction

The iterative correction is applied when there are severe artifacts on the initial image, and we expect the image quality to get better after each iteration. Basically, the idea is to repeat the previous procedures until a stopping criteria has been reached. The details are omitted here.

3. RESULTS

In this section, we demonstrate the effectiveness of the proposed method by numerical experiments on different types of image data, and provide qualitative and quantitative comparisons with other methods.

Fig. 4 shows how Euler's elastica inpainting works on the sinogram image. The metal trace is the region outlined by the red lines. The inpainting result is shown on the upper right image. We can see that sharp edges and the curvature of the original bands are well-preserved; see e.g. the locations indicated by the red arrows. The bottom four images are zoomed out regions from a head phantom. The comparison with the linear interpolation metal artifact reduction method, LIMAR (denoted by LI), and the cubic interpolation metal artifact reduction method, CIMAR (denoted by Cubic), clearly shows that Euler's elastica inpainting produces a much smoother result, while the other two methods create inconsistent lines within the inpainting region. Fig. 5 shows the performance

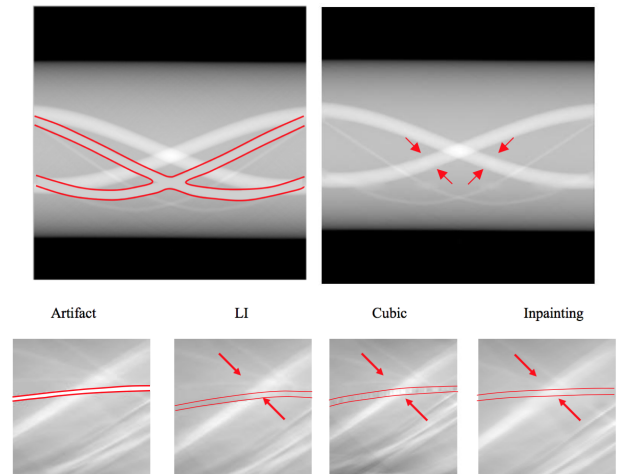


Fig. 4. Interpolation results on the sinogram given by the linear interpolation metal artifact (LIMAR), cubic interpolation metal artifact (CIMAR), and Euler's elastica inpainting.

between different MAR methods. In order for a fair comparison, we simulated similar artifact jaw images as in [11], and compare LIMAR and Inpainting results with the NMAR results in the original paper which are not shown here. All three methods are able to noticeably reduce streaking artifacts surrounding the tooth area. LIMAR reduces artifacts at the cost of introducing new artifacts at other locations. Both Inpainting and NMAR in the paper perform well in suppressing artifacts without creating new artifacts in other regions. NMAR works better when metal objects are smaller, while Inpainting performs well in all three cases.

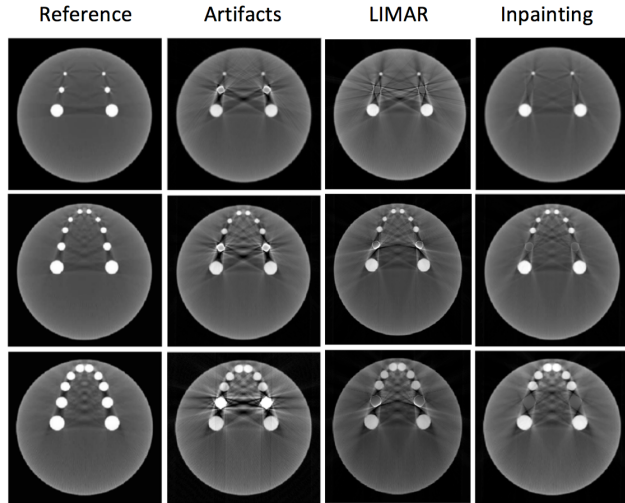


Fig. 5. Restoration results on jaw phantom images given by the LIMAR and Inpainting methods.

A quantitative evaluation (Table 1) is conducted with two measures: root-mean-square error (RMSE) and peak signal-to-noise ratio (PSNR). Small values of RMSE and large values of PSNR indicate better restoration results. We can see that Inpainting method consistently produces better quality results for all three phantom images. We have also compared

		LIMAR	Inpainting
Phantom1	PSNR	12.9329	16.2534
	RMSE	0.0234	0.0112
Phantom2	PSNR	7.2342	12.3523
	RMSE	0.0454	0.02865
Phantom3	PSNR	8.3563	12.6358
	RMSE	0.0314	0.02665

Table 1. Quantitative comparison of the LIMAR and Inpainting methods.

the different methods on clinical CT phantom images. Fig. 6 shows the artifact images of hip endoprosthesis, head implant, and dental fillings in column 1 and the restored image results given by the LIMAR, CMAR and Inpainting methods

in columns 2-4, respectively. From the comparison, it is apparent that the inpainting method yields the best restoration results among the three. Most of the streaking artifacts are suppressed, and the tissue structures of the background are preserved.

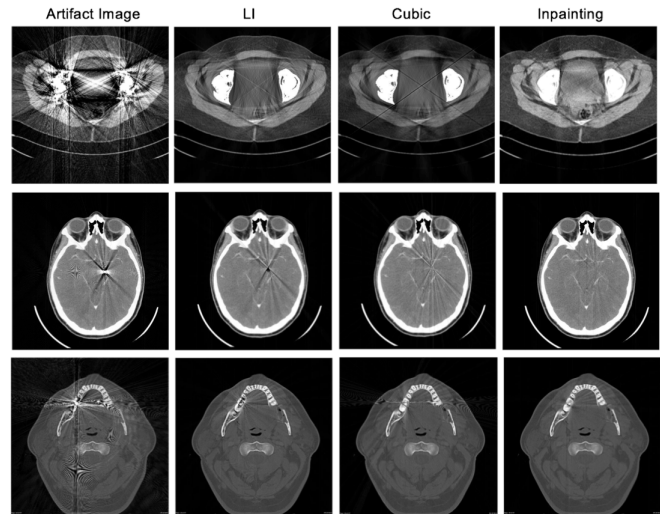


Fig. 6. Clinical CT phantom image comparison with the LIMAR, CIMAR, and Inpainting methods.

4. CONCLUSION

In this paper, we have proposed a novel method for metal artifact reduction based on Euler’s elastica inpainting. We observed a significant reduction of streak artifacts without introducing new artifacts in other regions; thereby, effectively improving the visual quality of CT images. A remarkable advantage of this approach is that it preserves sharp edges and curvature features of the sinogram image, thus resulting in much less artifact on the restored CT image. The Inpainting method has been compared favorably with the standard linear and cubic interpolation artifact reduction methods qualitatively and quantitatively on simulated and clinical images. The Euler’s elastica inpainting method consistently provides smoother and more accurate restoration results.

Future work includes improved segmentation, more accurate and efficient solution methods for solving the inpainting equation, and more extensive evaluation of the algorithms.

5. REFERENCES

[1] Mehrsima Abdoli, Rudi AJO Dierckx, and Habib Zaidi, “Metal artifact reduction strategies for improved attenuation correction in hybrid pet/ct imaging,” *Medical physics*, vol. 39, no. 6, pp. 3343–3360, 2012.

- [2] Willi A Kalender, Robert Hebel, and Johannes Ebersberger, "Reduction of ct artifacts caused by metallic implants.," *Radiology*, vol. 164, no. 2, pp. 576–577, 1987.
- [3] Mehrsima Abdoli, Johan R de Jong, Jan Pruim, Rudi AJO Dierckx, and Habib Zaidi, "Reduction of artefacts caused by hip implants in ct-based attenuation-corrected pet images using 2-d interpolation of a virtual sinogram on an irregular grid," *European journal of nuclear medicine and molecular imaging*, vol. 38, no. 12, pp. 2257–2268, 2011.
- [4] Mehrsima Abdoli, Mohammad Reza Ay, Alireza Ahmadian, and Habib Zaidi, "A virtual sinogram method to reduce dental metallic implant artefacts in computed tomography-based attenuation correction for pet," *Nuclear medicine communications*, vol. 31, no. 1, pp. 22–31, 2010.
- [5] Shiyong Zhao, DD Robeltson, Ge Wang, Bruce Whiting, and Kyongtae T Bae, "X-ray ct metal artifact reduction using wavelets: an application for imaging total hip prostheses," *IEEE transactions on medical imaging*, vol. 19, no. 12, pp. 1238–1247, 2000.
- [6] Esther Meyer, Rainer Raupach, Michael Lell, Bernhard Schmidt, and Marc Kachelrieß, "Normalized metal artifact reduction (nmar) in computed tomography," *Medical physics*, vol. 37, no. 10, pp. 5482–5493, 2010.
- [7] Marcelo Bertalmio, Guillermo Sapiro, Vincent Caselles, and Coloma Ballester, "Image inpainting," in *Proceedings of the 27th annual conference on Computer graphics and interactive techniques*. ACM Press/Addison-Wesley Publishing Co., 2000, pp. 417–424.
- [8] Jianhong Shen, Sung Ha Kang, and Tony F Chan, "Euler's elastica and curvature-based inpainting," *SIAM Journal on Applied Mathematics*, vol. 63, no. 2, pp. 564–592, 2003.
- [9] Jianhong Shen and Tony F Chan, "Mathematical models for local nontexture inpaintings," *SIAM Journal on Applied Mathematics*, vol. 62, no. 3, pp. 1019–1043, 2002.
- [10] Carlos Brito-Loeza and Ke Chen, "Fast numerical algorithms for eulers elastica inpainting model," *Int. J. Mod. Math*, vol. 5, pp. 157–182, 2010.
- [11] Abolfazl Mehranian, Mohammad Reza Ay, Arman Rahmim, and Habib Zaidi, "X-ray ct metal artifact reduction using wavelet domain sparse regularization," *IEEE transactions on medical imaging*, vol. 32, no. 9, pp. 1707–1722, 2013.